



Numerical Study about Effect of Different Boundary Conditions on Compressive Modulus Coefficient of Bonded and Non-Bonded Cylindrical Isolators

D Kamalakannan and B Prabu*

Department of Mechanical Engineering, Pondicherry Engineering College, Pondicherry 605 014, India

Received 29 August 2019; revised 05 February 2020; accepted 08 May 2020

Elastomers (Rubber and rubber-like materials) are widely utilized in many engineering applications due to their specific properties like high elasticity with good static and dynamic behaviors. Rubber blocks are one of the elastomeric components and it is employed in many applications such as vibration isolators, bumpers, shock absorbers, and dampers, etc. Most of the rubber blocks are cylindrical in shape and it can undergo large deformation under different loadings and contact conditions (fixed-fixed, friction-friction and fixed-friction). In this present work, experimentally validated Ogden hyper-elastic material model is adopted in the finite element analysis (FEA). The FE model is validated with other published experimental work. In addition, the following six boundary conditions namely BC1 (Fixed – Fixed), BC2 (Fixed – Friction), BC3 (Friction – Friction), BC4 (Fixed – Cap), BC5 (Cap – Friction) and BC6 (Cap – Cap) boundary conditions are taken for comparative study. The aspect ratio (radius/height) of the rubber isolator also varied as 0.5, 0.75, and 1. From the numerical analysis carried out, it is found that the BC6 (Cap–Cap) with aspect ratio 1 showed better compressive modulus coefficient over other parameters taken for study.

Keywords: Aspect ratio, Boundary conditions, FE analysis, Rubber isolators, Uniaxial compression

Introduction

The effect of different boundary conditions on compressive stiffness of cylindrical rubber isolator under static uniaxial compressive loading was derived by using analytical method.¹ Various hyper-elastic material models based on strain energy density (SED) functions are compared for the suitability of material models to predict uniaxial deformation test results.^{2,3} Nonlinear characteristics of static stiffness and ultimate behavior of rubber isolator under the different combined loading conditions were determined by using material stretch test, static load test, and FE analysis.^{4,5} Effect of material and thickness of rubber pads used in elastomeric isolator on shear modulus and compressive modulus were determined by using numerical method.^{6,7} Total stiffness of a rubber pad bonded between parallel rigid end-plates to determine bulk compressibility of the rubber isolator was studied by using closed-form solution procedure.⁸⁻¹⁰ In fact, to the best of the knowledge of authors, it is very clear that there is no FE simulation work to study the effect of different boundary conditions on the compressive modulus of

the cylindrical rubber isolator having nonlinear hyper-elastic material behavior.

Method proposed

While designing a rubber isolator, it is essential to determine the compressive modulus which in turn is affected by the shape, size, boundary conditions, and material model. The different boundary conditions considered in this present study are taken from reference Polukoshk *et al.*¹ and here they are named as: BC1 (Fixed – Fixed), BC2 (Fixed – Friction), BC3 (Friction – Friction), BC4 (Cap – Fixed), BC5 (Cap – Friction) and BC6 (Cap – Cap) as shown in Fig. 1. Efforts are taken to study the effect of different boundary conditions on the compressive modulus of rubber isolator subjected to uniaxial compression using the axisymmetric FE models of cylindrical rubber isolators are generated and analyzed using general-purpose FEA software ANSYS12. To account for the geometry of cylindrical rubber isolator, aspect ratio ($AR = r/h$; where, r -radius in mm, h -height in mm) is varied as 0.5, 0.75 and 1 and validated Ogden hyper-elastic material model is adopted in the FE analysis. The general equation of the hyper-elastic Ogden material model is given in Eq. (1) and

*Author for Correspondence
E-mail: prabu@pec.edu

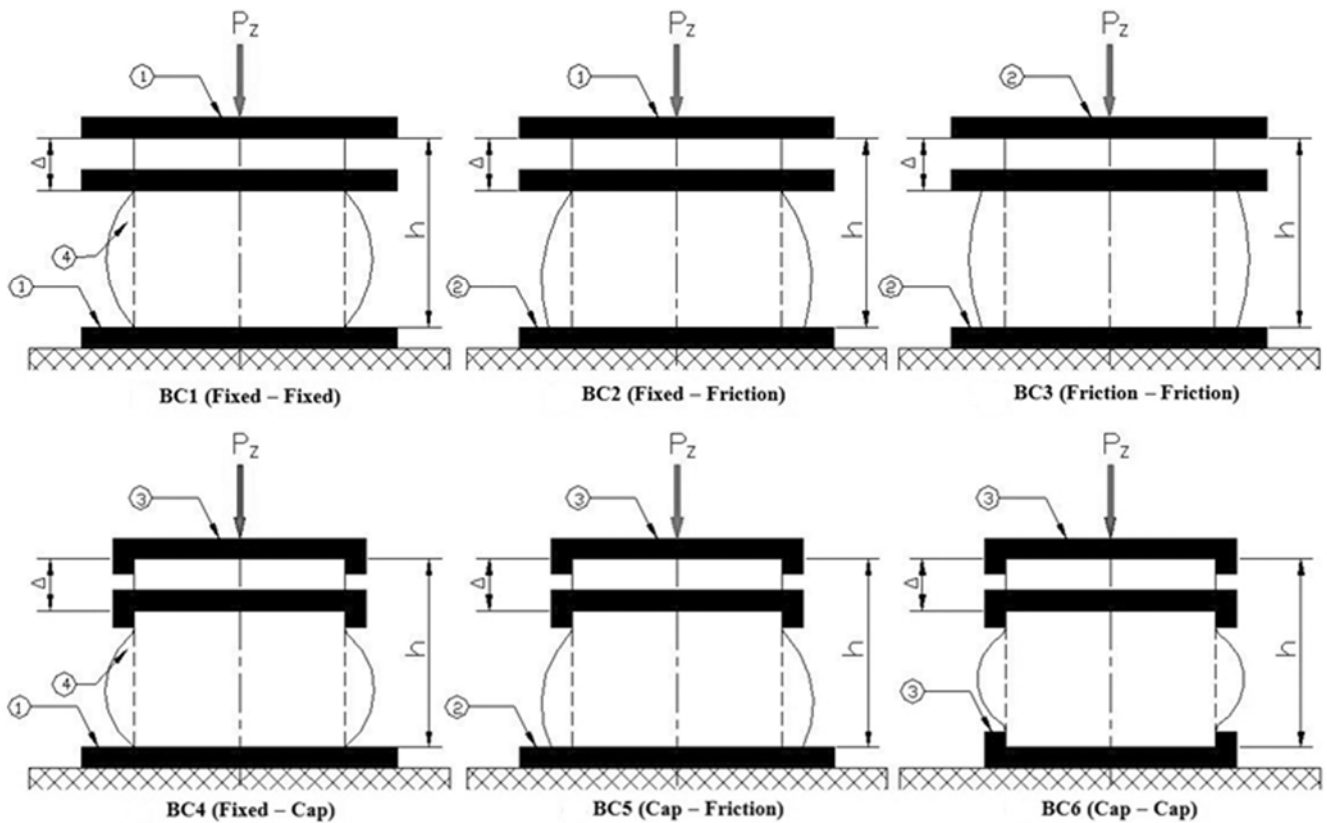


Fig. 1 — Different boundary conditions of cylindrical rubber isolator taken to study. where, (1) Fixed plate; (2) Friction plate; (3) Fixed cap and (4) Rubber block; h – The initial height of rubber block; Δ – Total axial displacement; P_z – Force in the z-axis

it is fitted with experimental test data using nonlinear regression analysis.

$$w = \sum_{n=1}^N \frac{\mu_n}{\alpha_n} (\lambda_1^{\alpha_n} + \lambda_2^{\alpha_n} + \lambda_3^{\alpha_n} - 3) \quad \dots (1)$$

where, the coefficients μ_n and α_n are material constants.

As all the stress-strain behavior of cylindrical rubber isolators with different boundary conditions under static uniaxial compressive loading are nonlinear in nature, the power-law model given in Eq. (2) is adopted to set the relationship between strain vs. compressive stress behaviors of rubber isolators.

$$y = k(x)^n \quad \dots (2)$$

where, k – modulus coefficient, n – power coefficient, x – strain and y – stress.

FE model validation

In order to validate FE analysis results, the experimental compressive load vs. displacement response of nitrile butadiene rubber with 30% of

carbon black³ for non-bonded (Friction–Friction) boundary condition having a coefficient of friction (μ) = 0 is taken for study. The fitted coefficients of fourth-order Ogden material model values obtained through nonlinear regression analysis is as follows: $\mu_1 = -0.3210$ N/mm, $\alpha_1 = 1.6014$, $\mu_2 = -0.2711$ N/mm, $\alpha_2 = 2.3046$, $\mu_3 = 0.0679$ N/mm, $\alpha_3 = 2.5694$, $\mu_4 = 0.5144$ N/mm, $\alpha_4 = 1.9546$. The radius of the cylindrical rubber block (r) = 14.5 mm and thickness (h) = 12.5 mm. The material properties of the steel end-plate are taken as Young's modulus (E) = $2.1E5$ N/mm², Poisson's ratio (ν) = 0.3 and mass density (ρ) = 7800 kg/m³. The axial compressive displacement (Δ) from 0 to 6 mm in steps of 1mm is applied to the FE model.³ PLANE182 elements are used for axisymmetric FE model of rubber block and steel plate portion of cylindrical rubber NBR isolator. PLANE182 element can handle hyper-elasticity, plasticity, stress stiffening, large deformation problems and also this linear quadratic element which has two degrees of freedom namely UX = translation along the x-direction and UY = translation along the y-direction. CONTA171 and TARGET169 elements

are also used to model the contact condition between the steel plate and rubber portion of the isolator. Deformed and un-deformed plot of non-bonded or BC3 (Friction–Friction) boundary condition under uniaxial compressive loading with a coefficient of friction (μ) = 0 is shown in Fig. 2 whereas Fig. 3 compares the experimental uniaxial compressive load vs. displacement test result³ with the present FE analysis result. From this comparison, it can be concluded that the present FE analysis provides accurate and reliable results.

Nonlinear FE analyses of different boundary conditions for HDR isolator

The different boundary conditions considered in this analysis, the initial height (h) of the rubber block is taken as 20 mm and the radius(r) varied from 10

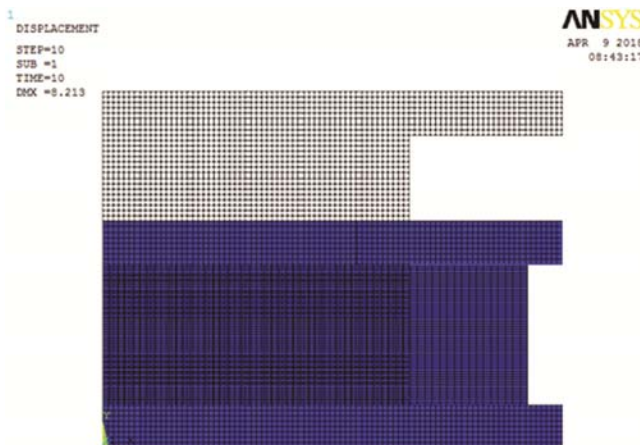


Fig. 2 — Deformed and un-deformed plot of BC3 (Friction–Friction) boundary condition with zero coefficient of friction

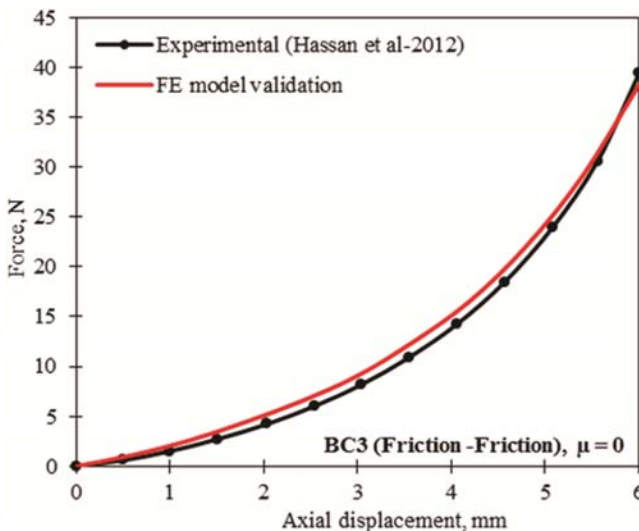


Fig. 3 — Comparison of experimental uniaxial compressive load vs. displacement result with present FE analysis result

mm to 20 mm in steps of 5 in order to vary the aspect ratio. In the present work, two types of end plates are used namely fixed end plates and friction end-plates and thickness of end-plates is taken as 2 mm. In the case of capped isolators, the top and bottom cap thickness and cap-height are taken as 2 mm and 3 mm respectively. In order to determine the compressive modulus of high damping rubber (HDR) isolator with different boundary conditions, third-order Ogden material model given in reference Iwamoto⁴ is taken for study and the material model coefficient values are as follows: $\mu_1 = 7.086E^{-01}$ N/mm, $\alpha_1 = 1.358$, $\mu_2 = 2.996E^{-06}$ N/mm, $\alpha_2 = 1.292E^{+01}$, $\mu_3 = -6.322E^{-03}$ N/mm, $\alpha_3 = -3.627$. The uniform axial compressive displacement load (Δ) from 0 to 7.2 mm in steps of 0.3 mm is applied on the different isolator FE models generated. The required axisymmetric FE models with different boundary conditions are generated following the procedure adopted in the previous section FE model validation. The axial-displacement contours at their ultimate load conditions of different boundary conditions of rubber isolator under static uniaxial compressive loading having an aspect ratio (AR) = 0.75 is shown in Fig. 4.

Results and Discussion

Through nonlinear regression analysis, power-law model equation is fitted to predict the compressive modulus coefficient and power coefficient values of all the isolators taken for the study. These compressive modulus coefficients and power coefficients of isolators have different aspect ratio such as (AR) = 0.5, 0.75 and 1 with different boundary conditions along with sum square error (SSE) values are given in Table 1. Sum square error values indicate that determinations of these coefficients are better as their values are nearer to zero. From case 1 of fixed boundary conditions given in Table 1, it is clear that the modulus coefficient and power coefficient are higher for BC6 (Cap–Cap) and lower for BC1 (Fixed–Fixed) compared with fixed boundary conditions having an aspect ratio (AR) = 0.75. Out of these three fixed boundary conditions, BC6 (Cap–Cap) shows higher modulus coefficient by 1.598 times that of the BC4 (Fixed–Cap) and 2.169 times that of the BC1 (Fixed–Fixed). From cases 2–4 given in Table 1, it can be understood that the modulus coefficient and power coefficient are higher for BC5 (Cap–Friction) and lower for BC3 (Friction–Friction). And also it can be noted that as the

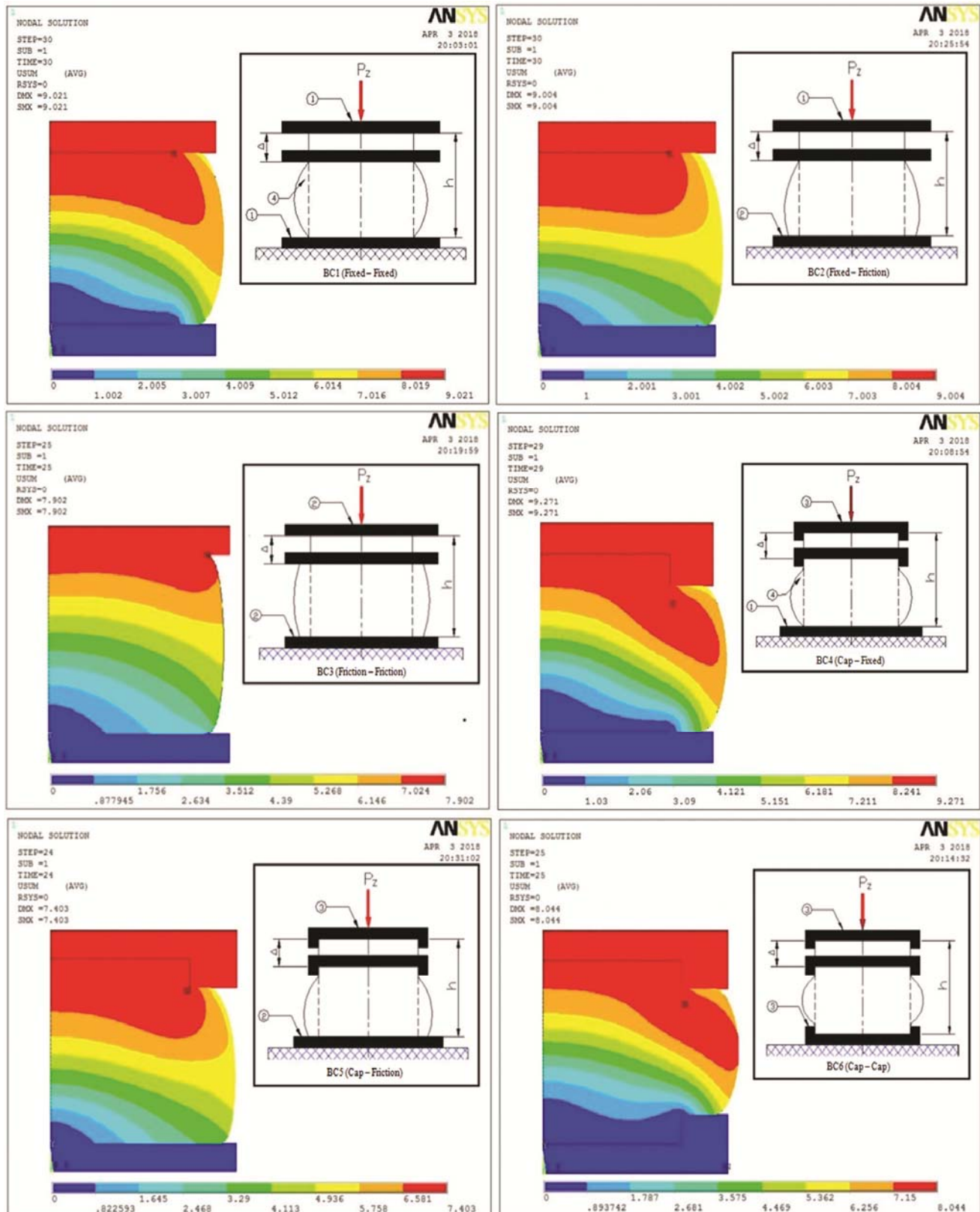


Fig. 4 — Axial-displacement contours at their ultimate load conditions of the different boundary conditions of cylindrical rubber isolator under static uniaxial compression using FE simulation

Table 1 — Uniaxial compressive modulus coefficient and power coefficient values are determined using the power-law model for different boundary conditions of HDR isolator

Case no.	Aspect ratio, AR = (r/h)	Boundary conditions, (BC)	Contact conditions		Powerlaw equation for nonlinear hyper-elastic Ogden model, $y = k(x)^n$		
			Fixed	Friction Coefficient of friction, (μ)	Modulus coefficient, k (N/mm ²)	Power coefficient, (n)	Sum square error, (SSE)
1	0.75	BC1 (Fixed–Fixed) BC4 (Cap–Fixed) BC6 (Cap–Cap)	Fixed	—	4.211	1.298	0.004
					5.714	1.395	0.018
					9.135	1.579	0.065
2	—	BC2 (Fixed–Friction)	—	0	3.621	1.303	0.002
				0.1	3.956	1.330	0.003
				0.2	4.204	1.340	0.004
				0.5	4.216	1.302	0.005
3	—	BC3 (Friction–Friction)	—	0	3.506	1.349	0.003
				0.1	3.813	1.355	0.003
				0.2	4.521	1.416	0.006
				0.5	4.616	1.359	0.010
4	—	BC5 (Cap–Friction)	—	0	4.419	1.344	0.004
				0.1	5.079	1.399	0.009
				0.2	5.625	1.429	0.012
				0.5	5.720	1.398	0.018
5	0.5	BC1 (Fixed–Fixed)	Fixed	—	3.748	1.295	0.002
	0.75				4.211	1.298	0.004
	1				5.465	1.365	0.015
6	0.5	BC4 (Cap–Fixed)	—	—	4.629	1.388	0.006
	0.75				5.714	1.395	0.018
	1				8.130	1.516	0.049
7	0.5	BC6 (Cap–Cap)	—	—	6.425	1.440	0.022
	0.75				9.135	1.579	0.065
	1				13.585	1.722	0.125
8	0.5	BC2 (Fixed–Friction)	—	0.1	3.675	1.316	0.002
	0.75				3.956	1.330	0.003
	1				4.277	1.343	0.006
9	0.5	BC3 (Friction–Friction)	—	—	3.651	1.344	0.002
	0.75				3.813	1.355	0.003
	1				3.990	1.367	0.003
10	0.5	BC5 (Cap–Friction)	—	—	4.543	1.360	0.004
	0.75				5.079	1.399	0.009
	1				5.510	1.412	0.013

coefficient of friction (μ) increases, modulus coefficient and power coefficient also increases. For example, in case of BC2 (Fixed–Friction) as the coefficient of friction (μ) increased from 0 to 1, the modulus coefficient also increased by 1.164 times. From cases 5–10 given in Table 1, it is clear that the modulus coefficient and power coefficient are higher for BC6 (Cap–Cap) and lower for BC3 (Friction–Friction) when compared with other boundary conditions. And also it is noted that as the aspect ratio increases, modulus coefficient and power coefficient

also increases. For example in BC1 (Fixed–Fixed), as the aspect ratio (AR) increased from 0.5 to 1 the modulus coefficient also increased by 1.458 times.

Conclusions

The following conclusions are derived from the numerical study carried out in the present work:

- 1 In case 1 of fixed boundary conditions, BC6 (Cap–Cap) shows higher compressive modulus and BC1 (Fixed–Fixed) shows lower compressive modulus.

- 2 In cases 2–4 of frictional boundary conditions, as the coefficient of friction (μ) increases the compressive modulus of rubber isolator also increases. Similarly in cases 5–10 of all the different boundary conditions, as the aspect ratio (AR) increases the load-carrying capacity of rubber isolator also increases.
- 3 Out of all different boundary conditions considered in this comparative study, BC6 (Cap–Cap) shows higher load carrying capacity as this boundary conditions provides better support to rubber block during loading and in contrast, BC3 (Friction–Friction) with the lowest coefficient of friction shows lower load-carrying capacity.

References

- 1 Polukoshko S, Gonca V, Martinovs A & Sokolova S, Boundary conditions influence on compressive stiffness of elastomeric isolators, *proceedings of the international scientific conference* (Latvia University of Agriculture), 2016.
- 2 Ali A, Hosseini M & Sahari B B, A review and comparison on some rubber elasticity models, *J Sci Ind Res*, **69(7)** (2010) 495–500.
- 3 Hassan M A, Abouel-Kasem A, El-Sharief M A & Yusof F, Evaluation of the material constants of nitrile butadiene rubbers (NBRs) with different carbon black loading (CB): FE-simulation and experimental, *Polym*, **53(17)** (2012) 3807–3814.
- 4 Iwamoto K, A Study on nonlinear characteristics of rubber isolator, *J Sys Design Dyn*, **5(5)** (2011): 1061–1076.
- 5 Zhou Tong, Wu Y-F, and Li A-Q, Numerical study on the ultimate behavior of elastomeric bearings under combined compression and shear, *KSCE J Civ Eng*, **22** (2018): 3556–3566.
- 6 Mishra H K, Akira Igarashi and Matsushima H, Finite element analysis and experimental verification of the scrap tire rubber pad isolator, *Bull Earthq Eng*, **11** (2013): 687–707.
- 7 Milani G, and Milani F, Behavior of Elastomeric Seismic Isolators Varying Rubber Material and Pad Thickness: A Numerical Insight, in *Simulation and Modeling Methodologies, Technologies and Applications*, by M Obaidat, J Filipe, J Kacprzyk and N Pina, *Advances in Intelligent Systems and Computing*, Springer, Cham, 256, 2014, 55–70.
- 8 Qiao S and Lu Nanshu, Analytical solutions for bonded elastically compressible layers, *Int J Solids Struct*, **58** (2015) 353–365.
- 9 Shi W, Liu G and Chen Z, Effects of the bulk compressibility on rubber isolator's compressive behaviors, *Adv Mech Eng*, **9** (2017) 1687814017699352.
- 10 Lesmana, Y and Sugihardjo H, Finite element study on vertical characteristic of modified circular perforated-reinforced elastomeric isolators (MC-PREIs), *Asian J Civ Eng*, **20** (2019) 21–33.